PPP for Advanced Precise Positioning Applications, Including Reliability Bound

Laínez Samper, María D., Romay Merino, Miguel M., Tobías González, Guillermo, Barba Martí, David, *GMV*

BIOGRAPHIES

María D. Laínez Samper is currently coordinating the GMV research activities in the field of Satellite Navigation, and in particular she is coordinating research activities in the field of precise positioning applications. She has also worked in experimentation and verification activities, in the Operational Systems Division, during the preliminary phases of the Galileo Program, and has been the responsible for the clock prediction and navigation message computation modules in the Galileo E-OSPF (Experimental Orbitography and Synchronization Processing Facility).

Miguel M. Romay Merino is the GNSS Business Unit Director at GMV Aerospace and Defence. Miguel leads the GMV Unit that has become one of the strongest groups of GNSS experts thanks to its key involvement in GPS, EGNOS and Galileo. Miguel has been a pioneer in the Galileo Program, collaborating on aspects such as constellation design, precise orbit determination, integrity, performance evaluation, system definition, etc. Miguel is today involved in GMV research activities in the definition of novel GNSS applications and on the design of new generation GNSS. Miguel has been recently nominated Chairman of the EC MEAG.

Mr. Guillermo Tobías González holds an MSc in Telecommunication Engineering by the University of Zaragoza. Since joining GMV, he has actively participated in different projects within the GNSS Business Unit and he has been always linked to the development and exploitation of the magicGNSS suite as well as involved in R&D activates related to high accuracy positioning. Specialized in the development and experimentation of GNSS algorithms for GPS and Galileo, he has been the GMV's responsible for the magicGNSS suite for the last years and he has led the definition different GNSS services and GNSS products provided by GMV for precise positioning. He is currently coordinating R&D activities related to PPP services and he is the technical manager for the development of the Galileo Commercial Service Demonstrator, which will include the provision of a HA service.

David Barba Martí holds an MSc in Aeronautical engineering from Polytechnic University of Valencia, specialty in Aircraft and Spacecraft. After graduation David Barba joined GMV as project engineer. Since then, he has been working as GNSS engineer at the GMV GNSS Business Unit performing related activities with magicGNSS, a suite of tools for GNSS data processing featuring high-precision and integrity.

ABSTRACT

The PPP technology is able to complement the basic GNSS functionalities for providing an advanced high accurate PNT solution. PPP algorithms use code and phase observations from a dual-frequency receiver, together with precise satellite orbits and clocks, in order to calculate high accurate receiver coordinates and precise clock estimations. Our GNSS team has developed the algorithms and the infrastructure, except for the tracking network, needed for providing a commercial PPP service. We can manage all the required components, from the real time orbit and clock products generation, to the PPP filter implementation and the service provision. As a differentiating feature, we are working on providing a reliability bound, together with accuracy, continuity and availability to our PPP solution, which we think will help widening its applicability range.

In this paper we are going to analyze the PPP problem, trying to understand which the essential limitations of the process are. We are going to consider in detail the GNSS constellations geometrical effects and how the quality of the orbit and clock products can affect the accuracy of the provided positioning solution. In addition to that, we are going to anayse the feasibility of providing the users with a dedicated correction built at server level in order to palliate the mentioned effects and we have been able to take one more step in the definition of a reliability bound for PPP. We are working in laying down the foundations for an upper-level reliability concept for PPP, closely linked to the final user perspective.

We aim at achieving the challenging task of enabling a wide range of GNSS uses, those involving high positioning accuracy, as well as those in which a certain reliability bound is required.

INTRODUCTION

Different technologies based on GNSS (alone or augmented and/or hybridized) are currently being used for many different applications. GPS and GLONASS are operational systems, and Galileo and Beidou are now being deployed. Augmentation systems such as WAAS,

EGNOS, MSAS and GAGAN are providing improved accuracy and integrity over the basic GNSS navigation solutions, and SDCM is progress. RTK, PPP and the integration with sensors, mapping data, local ionospheric information and other non-GNSS signals are allowing the achievement of excellent accuracy and reliability levels, and spreading the application of GNSS based technologies to many different fields. The receivers market is continuously evolving, incorporating innovative features as the systems are being developed and improved, for being able to provide a wider and wider range of positioning navigation solutions to a growing community of users.

PPP is one of the mentioned technologies which are able to complement the basic GNSS functionalities for providing an advanced PNT solution. The PPP algorithm is fed by both code and phase observations from a dual-frequency receiver, together with precise satellite orbits and clocks, in order to calculate high accurate receiver coordinates and precise clock estimations. The PPP filter process observations coming from the navigation satellites, and solves for different unknowns: receiver coordinates, receiver clock, zenith tropospheric delay and the phase ambiguities. Our GNSS team has developed the algorithms and the infrastructure, except for the tracking network, needed for providing a commercial PPP service. We can manage all the required components, from the real time orbit and clock products generation, to the PPP filter implementation and the service provision. As a differentiating feature, we are working on providing a reliability bound, together with accuracy, continuity and availability to our PPP solution, which we think will help widening its applicability range.

In addition to the system level integrity layer, which is aimed at preventing the user from a series of general failures, we are concerned about specific local effects at user level which can cause the final PNT solution to be inaccurate, even though the system is working normally. Several user level integrity/reliability (accuracy bound for non-aeronautical users) concepts have been formulated, being RAIM (receiver autonomous integrity monitoring) and its variants the most popular ones. It would be interesting to find an optimum combination of all significant sources to be used for building a reliability protection level aimed at bounding the user positioning error complying with certain confidence requirements tightly related to the final application.

In this paper we are going to analyze the PPP problem, trying to understand which the essential limitations of the process are. We are going to consider in detail the GNSS constellations geometrical effects and how the quality of the orbit and clock products can affect the accuracy of the provided positioning solution. Our objectives are:

- to identify potential accuracy improvement margins
- to analyze the feasibility of building a dedicated correction at server level to be delivered to be users for mitigating the effects of the geometry and the quality of the orbit and clock products on the position solution
- to define reliable error bounds for the provided positioning solutions

We do already have a strong background in this area. We have already been working with a reliability concept for *magicPPP*, our in-house developed PPP platform. We started by detecting different failure modes, following a practical service oriented approximation, paying particular attention to cases in which the PPP solution exceeded the expected accuracy bounds (in the centimeter magnitude order). We correlated those cases with indicators either at system or at user levels which could be considered to be significant for building a reliability bound. With PPP horizontal accuracy performances in the 5 to 10 cm range (95%) and vertical accuracy performances in the 10-20 centimeters range (95%), after a 15 to 30 minutes convergence period, preliminary protection levels better than 30 cm for the horizontal component and better than 50 cm for the vertical component were obtained. We have continued performing accuracy versus reliability analyses, and have observed that a combination of poor geometrical conditions together with slightly inaccurate orbit and clock products (which can be the case for real time products) can cause a significant growth of the PPP positioning errors. Consequently, we have decided to analyze the feasibility of providing the users with a dedicated correction built at server level in order to palliate the mentioned effects and we have been able to take one more step in the definition of a reliability bound for PPP. We have improved it by better fitting the uncertainty level of the PPP solution in order to mitigate the observed risk. The upcoming multi-constellation scenario is expected to be highly advantageous for PPP performances. *magicPPP* algorithms, initially prepared for GPS and GLONASS, have been enhanced for Galileo. Dedicated experimentation campaigns will be carried out for testing the multi-constellation algorithms feasibility in open sky, sub-urban and urban scenarios.

We are working in laying down the foundations for an upper-level reliability concept for PPP, closely linked to the final user perspective, which might open a new field for GNSS applications. The current demand for high precision GNSS based applications and services will keep on increasing in the next years. We aim at achieving the challenging task of enabling all these present and future GNSS uses, those involving high positioning accuracy, as well as those in which a certain reliability bound is required.

THE PPP TECHNIQUE AND *magicPPP*

PPP is a position location process which performs precise position determination using iono-free measurements, obtained from the combination of undifferenced, dual-frequency observations coming from a single GNSS receiver, together with detailed physical models and

corrections, and precise GNSS orbit and clock products calculated beforehand. The quality of the reference orbits and clocks used in PPP is critical, as it is one of the main error sources of the positioning solution. Apart from observations and precise reference products, PPP algorithm also needs several additional corrections which mitigate systematic effects which lead to centimetre variations in the undifferenced code and phase observations, for example phase wind-up corrections, satellite antenna offsets, station displacements due to tides (earth and oceanic), etc.

At a given epoch, and for a given satellite, the simplified observation equations are presented next:

$$l_p = \rho + c(b_{Rx} - b_{sat}) + Tr + \varepsilon_p \quad (1)$$

$$l_\phi = \rho + c(b_{Rx} - b_{sat}) + Tr + N\lambda + \varepsilon_\phi \quad (2)$$

Where:

- l_P is the ionosphere-free combination of L1 and L2 pseudoranges
- l_ϕ is the ionosphere-free combination of L1 and L2 carrier phases
- b_{Rx} is the receiver clock offset from the reference (GPS) time
- b_{Sat} is the satellite clock offset from the reference (GPS) time
- c is the vacuum speed of light
- Tr is the signal path delay due to the troposphere
- λ is the carrier combination wavelength
- N is the ambiguity of the carrier-phase ionosphere-free combination (it is not an integer number)
- ε_P and ε_ϕ are the measurement noise components, including multipath and other effects
- ρ is the geometrical range between the satellite and the receiver, computed as a function of the satellite (x_{Sat}, y_{Sat}, z_{Sat}) and receiver (x_{Rx}, y_{Rx}, z_{Rx}) coordinates as:

$$\rho = \sqrt{(x_{sat} - x_{Rx})^2 + (y_{sat} - y_{Rx})^2 + (z_{sat} - z_{Rx})^2} \quad (3)$$

The observations coming from all the satellites are processed together in a process that solves for the different unknowns; the receiver coordinates, phase ambiguity terms, the receiver clock offset and the zenith tropospheric delay. Most implementations of PPP algorithms use a sequential filter in which the process noise for the coordinates is adjusted depending on the receiver dynamics, the time evolution of the clock is more or less unconstrained (white noise with a high sigma), and the process noise for the tropospheric delay is adjusted to standard tropospheric activity. In the case of phase ambiguities, they are considered as a constant per pass. Other implementations feature a batch algorithm instead, and therefore no process noise has to be modelled. In this case, the receiver clock offset is estimated at every measurement epoch, the coordinates are adjusted for the entire observation interval (static mode) or per epoch (kinematic mode), the troposphere is estimated at regular fixed intervals and the ambiguities are also estimated per pass.

PPP is not a differential technique, it provides absolute positioning. On the one hand, integer carrier phase ambiguities cannot be obtained immediately after the PPP process has started (as it can be done for precise relative positioning techniques, i.e. RTK). PPP requires longer observation times for ensuring convergence has been achieved. On the other hand the PPP provided positioning solution is absolute, which can be a great advantage for many applications. The accuracy of RTK technique for absolute positioning applications has to be estimated combining the RTK positioning technique accuracy and the accuracy of the known position of the base station.

PPP has been normally conceived as a global service, taking into account that the orbit and clock products are themselves global. However, regional PPP services can also be provided, by feeding the PPP process with orbit and clock products generated from a non-global tracking network.

GMV has developed a proprietary PPP solution, which is called *magicPPP*, and provides an off-line PPP service as well as a RT PPP service. The PPP reference products generation is a complex process, especially for the demanding real time *magicPPP* service. The off-line *magicPPP* service is fed with products automatically generated processing data from a network of around 50 worldwide. The real time products generation process retrieves, from a worldwide station network, via Networked Transport of RTCM via Internet Protocol (www.rtcm-ntrip.org), NTRIP, dual-frequency code and phase measurements in real time. A high-level layout of the real time reference products generation infrastructure developed by GMV is shown in the figure below:

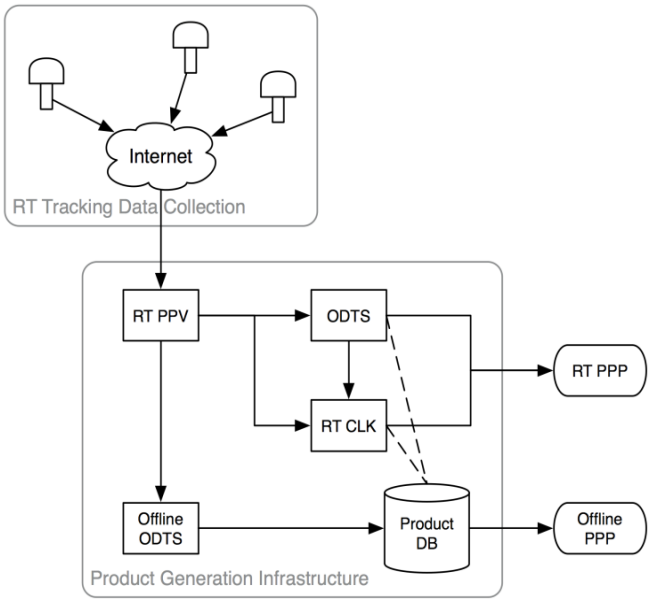

Figure 1: RT Product generation infrastructure

The reference product generation is based on an Orbit Determination and Time Synchronisation (ODTS) process. The GMV proprietary tool in charge of this process is *magicODTS*, which is part of the *magicGNSS* suite. *magicGNSS* is an OD&TS web tool (see http://magicgnss.gmv.com), able to compute multi-GNSS products.

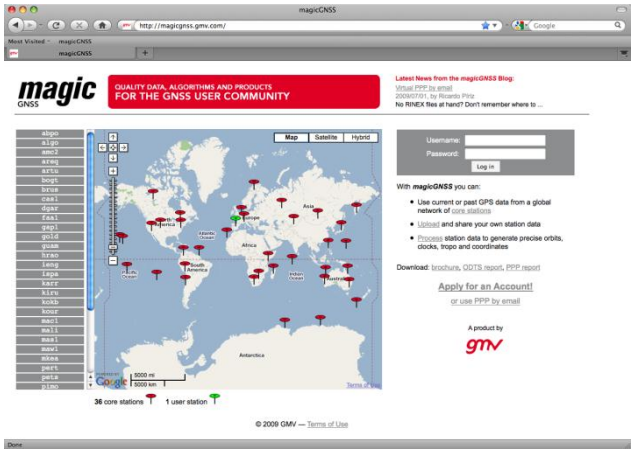

Figure 2: *magicGNSS* OD&TS tool

See [Ref. 3.] and [Ref. 4.] for further information about *magicGNSS*.

Back in 2010, GMV started participating as Analysis Centre for the Real Time IGS Pilot Project (http://www.rtigs.net/index.php), by processing data from a worldwide network of stations and providing precise predictions of GPS and GLONASS orbits and clocks, which are calculated using magicGNSS. Its contribution is still ongoing once Real Time IGS Project became operational in 2012. Both GPS and GLONASS are processed simultaneously. GLONASS inter-channel biases are estimated in order to compensate for the different internal delays in the pseudorange measurements through the GLONASS receiver, associated to the different frequencies used by the different satellites. Standard 2-day-long ODTS processes are executed every 15 minutes in order to generate real time orbit predictions, whereas real time clock data are generated at 1 second execution rate, via an auxiliary RT_CLK process, which estimates the satellite clocks in real time taking as input the pre-processed observations coming from PPV and the outputs from the last ODTS execution. The real-time orbits and clocks generated this way can be used for feeding *magicGNSS* RT PPP processes, and can be stored in standard formats (SP3, clock RINEX) for post-processing analyses.

As shown in Figure 1, the *magicGNSS* products generation includes the execution of an offline ODTS process which runs in off-line post-processing mode with a latency of 2 days and specific setup. It generates orbit and clock products more accurate than the real time ones. When available, they can be used for feeding off-line PPP processes.

The comparison of the off-line products, orbits and clocks, with IGS is shown in Figure 3. Typical orbit accuracy is about 6 cm, RMS, and clock accuracy is about 0.25 ns, RMS. For GLONASS, the analogue comparison has been carried out by comparing the off-line *magicGNSS* products with respect to ESOC (European Space Operations Centre) products. The orbit RMS stays around 10 cm, and the clock RMS stays around 0.4 ns, as shown in Figure 4.

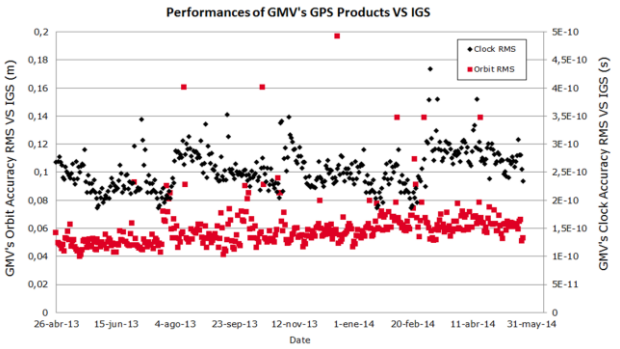

Figure 3: GPS Orbit and Clock comparison between IGS products and off-line magicGNSS products for April 2013-June 2014

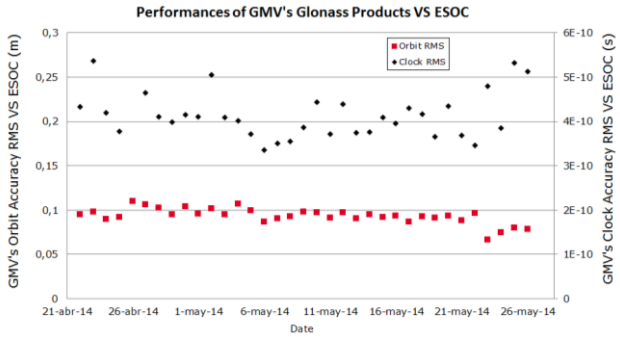

Figure 4: GLONASS Orbit and Clock comparison between ESOC products and off-line magicGNSS products for April 2013-June 2014

magicGNSS does also process Galileo data. Precise orbit and clock products can be computed, and fed into PPP processes. The first PPP results obtained with *magicPPP* with Galileo are reported in [Ref. 6.]. See [Ref. 5.] and [Ref. 6.] for further information about the *magicPPP* off-line and real time services.

magicPPP PERFORMANCES

The performances of *magicPPP* are going to be described in the next paragraphs, off-line and real time static and dynamic scenarios have been considered.

Off-line Static Performances

The following figures illustrate the performances of the *magicPPP* off-line service for static scenarios for different processed data intervals, ranging from 15 minutes to 24 hours.

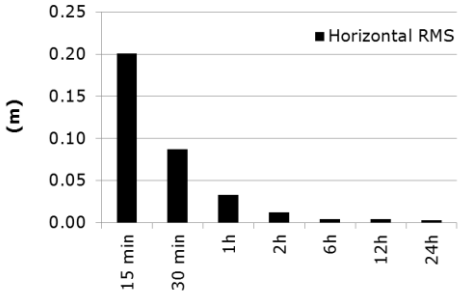

Figure 5: Static off-line performances - Horizontal

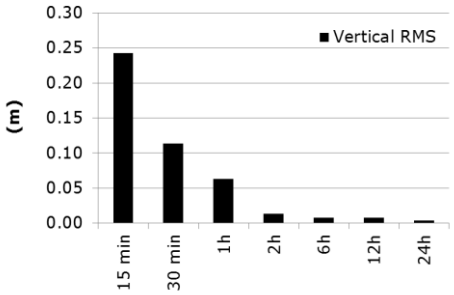

Figure 6: Static off-line performances - Vertical

The test was carried out with IGS RINEX multi-constellation data (GPS + GLONASS) from eight different stations (brux, dakr, flsrs, graz, madr, riga, roap and tro1), and off-line orbit and clock products generated by *magicODTS*. A 48 hours interval was processed with *magicPPP*, covering days 134 and 135 in 2014 (May 14th and 15th) in order to get a set of precise reference coordinates. An analogous PPP process was carried out but fed with orbit and clock products from IGS, in order to have an estimation of the accuracy of the obtained precise reference orbits. The differences between the two sets of coordinates was carried out, and the RMS of the differences was found to be below 1 cm. Different PPP processes were then carried out for the different data intervals (15 min, 30 min, 1h, 2h, 6h, 12h and 24h), and the obtained coordinates for the different data intervals were compared with respect to the ones previously obtained for the 2-day-long data set. The above plots show the RMS of the eight considered stations. Horizontal accuracy below 10 cm and vertical accuracy below 15 cm (RMS) are obtained after a 30 minutes long convergence period. Accuracies below 5 cm are obtained for 2-hour-long intervals and longer. These results illustrate the good quality of the reference off-line products as well as the accurate performances of the off-line static *magicPPP* algorithm.

RT Static Performances

magicPPP RT static performances are going to be described in this subsection. 160 days have been processed, starting from January 31st until July 9th 2014, slightly more than 5 months. A total of 62 hours have been excluded from the mentioned analyses, representing a 1.61% unavailability period of the total analysed interval. These 62 hours include both internal and external events, such as incidences in the communications, a database exception and the GLONASS outages (April 1st and 14th, 2014). The reported 1.61% unavailability is a rather good performance, which could still be improved by setting additional operational requirements to the testing platform we have used for the present analyses.

The following figures have been elaborated, showing the horizontal and vertical errors, obtained by comparing the obtained PPP position solution with respect to the calibrated coordinated of the reference station (GAP1). Figure 7 and Figure 8 below show the obtained horizontal and vertical obtained values (cm).

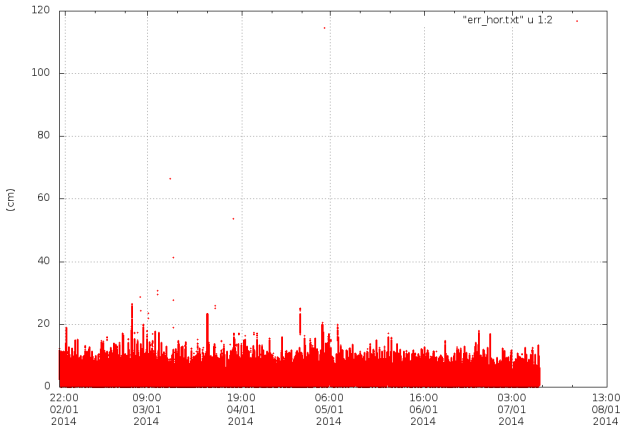

Figure 7: RT static PPP horizontal accuracy

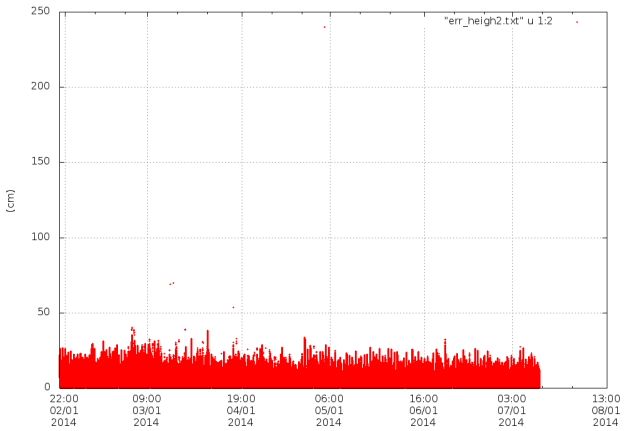

Figure 8: RT static PPP vertical accuracy

Together with the PPP positioning solution, a horizontal and a vertical bound can be provided, see [Ref. 6.]. The provided reliability indicators or protection levels (PL_H, PL_V) have been computed taking into account the following factors:

- Constant term for compensating the uncertainty associated to the definition of the reference frame.
- Covariance indicators coming out from the PPP estimation filter
- Residuals of the position estimation process
- Additional margin aimed at compensating for the strong correlations during the initial convergence period.

The obtained horizontal and vertical reliability bounds or PLs are shown in Figure 9 and Figure 10 below:

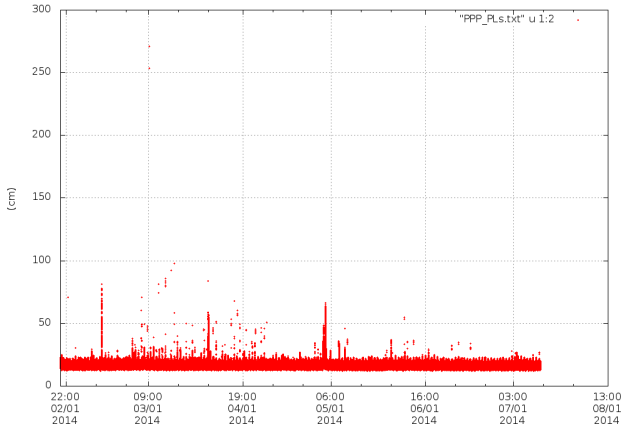

Figure 9: RT static PPP horizontal reliability bound

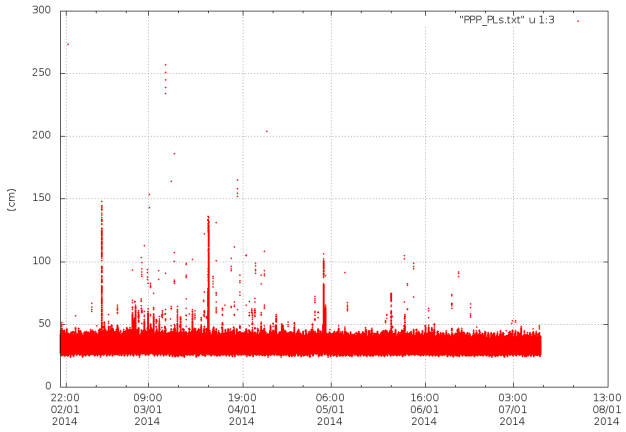

Figure 10: RT static PPP horizontal reliability bound

The followed strategy for the reliability bound computation is the same as the one implemented for the tests reported in [Ref. 6.]. The analysis of the results obtained in this broader campaign is going to be used for improving the reliability bound computation algorithm. The results obtained with the improved reliability bound computation strategy are presented in the last section in this paper. For a better understanding and interpretation of the figures above, a table showing the horizontal and vertical PPP positioning errors and the associated reliability bounds statistics, including different percentiles, has been elaborated:

Table 1: RT static PPP performances

Percentile	|H_Err| (cm)	|V_Err| (cm)	PL_H (cm)	PL_V (cm)
68.268949	4.89	6.70	16.85	32.82
95.449973	8.67	14.7	18.79	37.42
99.730020	14.04	22.7	22.09	42.30
99.993665	21.97	32.00	51.96	87.31
99.999942	23.38	39.05	82.00	180.00
99.999999	114.53	240.00	271.21	273.44

The obtained results are certainly promising. 95% of the times the horizontal error is below 10 cm, and the vertical error below 15 cm, whereas the reliability bounds remain below 20 cm and below 40 cm, respectively. Even for very high percentiles, PPP provided positioning errors stay below 0.5 m and the associated reliability bounds below 1 metre. And still there is margin for improvement. We are going to pay attention to the reliability failure epochs and we are going to critically analyse the PPP process and context, in order to understand what can limit its performances. We will see in subsequent paragraphs and sections different improvement factors which will contribute to the enhancement of the already good PPP positioning accuracy and associated reliability levels.

More than 13.5 million epochs from January 31st until July 9th 2014 have been processed, and the associated classic Stanford diagrams have been generated. They are shown in Figure 11and Figure 12 below:

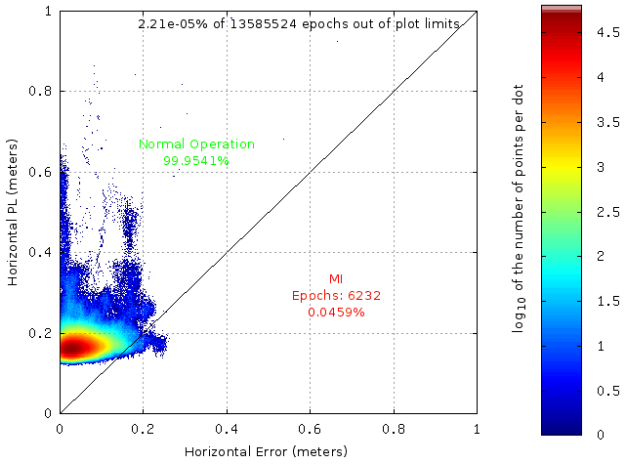

Figure 11: PPP reliability algorithm, horizontal component - Stanford diagram

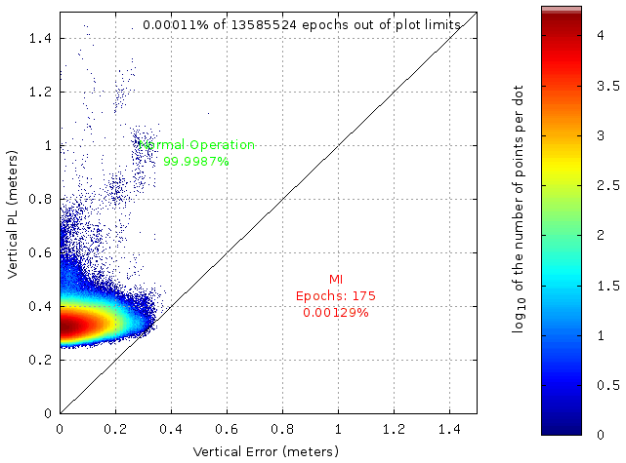

Figure 12: PPP reliability algorithm, vertical component - Stanford diagram

It can be observed that protection levels below 1 m for the horizontal error component and below 1.5 m for the vertical error component are obtained most of the times. Just an almost negligible percentage of times 2.21e-05%

and 1.1e-04% of times the obtained reliability bounds are larger than those stringent limits. With the mentioned reliability computation algorithm, several integrity failures can be observed, especially in the horizontal error component. However, the Stanford diagrams in Figure 11 and Figure 12 above show that in any the reliability failures exceed the bounding limit by far. Slightly higher reliability bounds would have provided reliable protection levels in most or all or the cases. The observed failures are going to be further investigated in order to minimise them, trying to reach the highest achievable reliability performances. Analogous analyses with the improved reliability computation algorithm are presented in the last section in the paper, showing enhanced reliability performances.

The following figures (Figure 13 and Figure 14) show the negative margins between the provided reliability bounds and the measured errors, as a function of time, for all the epochs at which a reliability failure has been detected, except for the 2014/04/29 09:07:32 anomaly. Including it would have required larger axes, which would have resulted in unclear plotting of the results. The reliability bound computation has been improved in order to cope with these integrity failures. The results are presented in the subsequent "Improved *magicPPP* Reliability Bound" section.

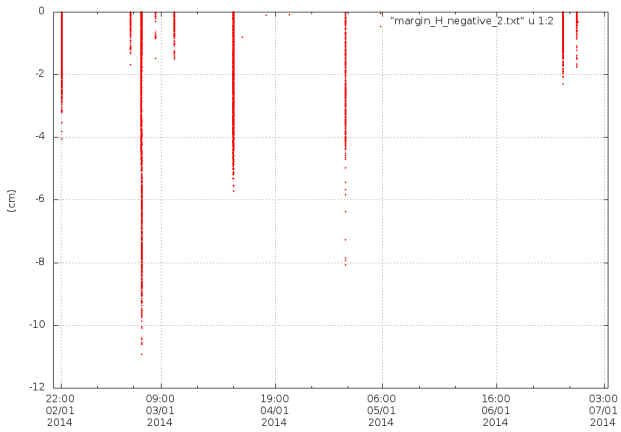

Figure 13: Horizontal reliability failures magnitudes

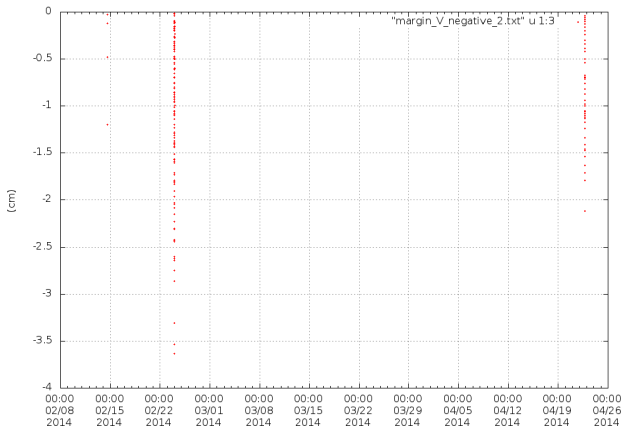

Figure 14: Vertical reliability failures magnitudes

The analysis of the reliability failures can be associated to periods at which the PPP error was larger than usual in at least one of the components. As an example, we are going to illustrate what happened on 2014/02/02, around 04:00:00. Around that epoch, the horizontal error in the east-west component was larger than 10 cm, see Figure 15, and the horizontal reliability bound was slightly below than necessary. The cause of the observed unusually large errors in the PPP provided solutions can be attributed to a combination of the following two factors:

- inaccurate orbit and/or clock products and
- weak geometry.

What we mean by "inaccurate orbit and clock products" is that the orbit and clock error are slightly worse than the typical values, something like 20 cm in the orbit error, instead of 6 cm, or 0.45 ns instead of 0.25 ns in the clock error, see Figure 3, i.e. orbit and clock errors in the tails of the products error distributions. PPP positioning solutions can range in a decimetric band, but that it is extremely improbable that these decimetric bands are exceeded, once the process has converged. The OD&TS process is a like a first filter and the PPP process is a second filter, able to reject faulty satellites or stations. Dramatically wrong products can never be generated in a standard OD&TS process, and the PPP process I able to reject wrong products as long as the geometric conditions allow it. This is why only "slightly inaccurate" products can "contaminate" the PPP provided solution.

When the number of available satellites for the PPP computation is lower than this threshold, we have a risk of "weak geometry". When the number of satellites in view available for PPP is five or less, the PPP algorithm may not have the capability to detect and reject a satellite whose orbit and/or clock products have large errors. This happens when the DOP of the remaining non-faulty satellites is too large. When analysing a certain constellation geometry for PPP, we will pay attention to the minimum number of satellites in view, and to the maximum DOP of the constellation considering one satellite failure. Note that no reliability bound in provided in "weak geometry" conditions, i.e. when the number of satellites in view is less or equal than 5.

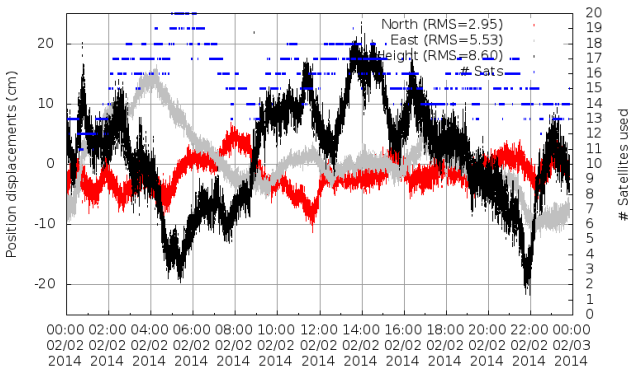

Figure 15: PPP position displacements (cm)

In conclusion, the mentioned degradation factors, the quality of the orbit and clock products as well as the navigation satellites geometry, can affect the accuracy of the positioning solution, but it is not easy to provide a direct quantitative estimation of their net effect on the PPP positioning solution. Hence we suggest doing it indirectly through a dedicated correction generated at server level to be delivered to the users for mitigating the mentioned effects. The navigation satellites geometry and the quality of the orbits and clock products will be further analysed and their effects described in more detail in subsequent dedicated sections. An improved reliability bound algorithm, indirectly considering the mentioned degradation factors will be introduced, and it will be tested and compared with respect to the original reliability bound computation implementation.

RT Kinematic Performances

It is important to note that the main difference between static and dynamic scenarios is not directly related to the fact that the receiver is moving. For the PPP algorithm, it is the same if the receiver position is changing or not. The only difference is related to the environment conditions, such as signal blockage (buildings or trees), multipath, communication losses, etc. which may cause the PPP algorithm performances to degrade, due to lack of observability and/or convergence loss.

No additional dedicated tests have been processed for showing the *magicPPP* performances in a real-time kinematic scenario. Previously obtained results can be consulted reported in [Ref. 6.], for open-sky, sub-urban and urban environments. The obtained results show that, in line with the theory, open-sky kinematic performances are comparable with those obtained for static open-sky conditions. Differences arise when lines of sight are lost, in partially obstructed scenarios. In those cases, the attainable accuracy levels degrade significantly, and local effects are also relevant for building a reliable error bound (in case the number of satellites in view is high enough, and it is feasible to build such a bound).

In view of the obtained results, we conclude that it could make sense to define two different PPP particularizations, one for open-sky, and another one for partially obstructed scenarios. Local effects have a much greater impact on the partially obstructed scenario, whereas the open-sky solution is mainly affected by the constellation geometry and the quality of the orbit and clock products. Increasing the robustness of the PPP solution, even if compensated with a relaxation of the accuracy requirements, would be very helpful in partially obstructed environments. Some different ideas can be suggested for enhancing the PPP robustness: among which we can mention the use of low cost receivers equipped with high sensitivity chip sets rather than more sophisticated geodetic receivers, a PPP mono-frequency approach, and the integration of PPP with inertial sensors. The two particularised PPP technologies would thus be able to fulfil different requirements set covering a wide range of applications, in the two mentioned scenarios: open-sky and semi-obstructed.

Off-line Kinematic Performances

One of the RT Kinematic Performances scenarios reported in [Ref. 6.] has been re-processed off-line, using post-processed orbit and clock products, and the obtained results have been compared with respect to the ones previously obtained using real time products. It corresponds to a relatively open sky environment with a RTK reference station in the vicinity. Some communication losses were forced to test the performance of the algorithm under these conditions. This example could illustrate the case in which for a certain application, the real-time requirement would not apply. In this case, it could probably make sense, if possible, to wait until more accurate post-processed products were available. The following figures show the errors in the horizontal and vertical component for this part of the trajectory, both for the real-time and off-line processes.

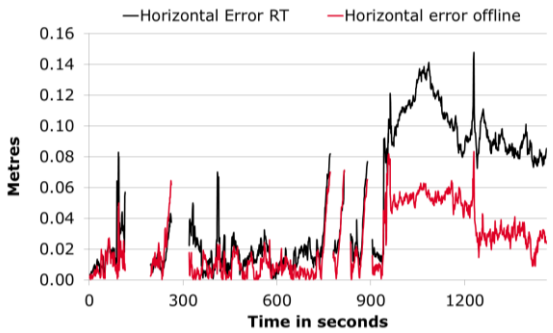

Figure 16: Horizontal error, real-time and off-line processes.

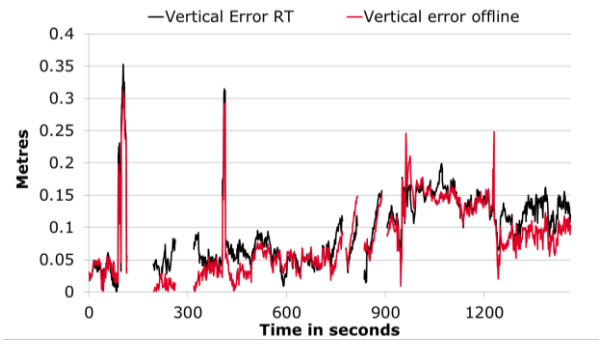

Figure 17: Vertical error, real-time and off-line processes.

Slightly better results can be observed in Figure 16 and Figure 17 above when off-line products are used. However the improvement is small, even in relatively benign conditions. In a more demanding partially obstructed scenario, the improvement of the quality of the orbit and clock products would have barely affected the PPP positioning solution. In this case, the main error factor would have been the loss of sight lines caused by trees or buildings.

magicPPP PERFORMANCES LIMITATIONS

We can summarise the results of the analyses of the *magicPPP* performances presented in the preceding sections, and say that it is a combination of the orbit and clock products quality together with GNSS constellation geometry what sets the bounds of the attainable PPP accuracy performances, especially in open-sky environments. It has to be noted that this geometry-products combination is also related to the PPP process convergence.

Since we started analysing our very first PPP tests, we found that the time the PPP solution took to stay below certain centimetric accuracy level, when observed in different PPP executions, was not homogeneous. The PPP solution does not follow a random distribution, but a repeatable pattern given by the observability conditions and the products quality, and when a process is started in a "badly conditioned" interval, the PPP solution converges, in a 15-30 minutes range, to a biased position, the same position that would have reached a different PPP process, which would have been started well in advance. This converged position will be close enough to the pre-calibrated reference position, as long as the geometry-products combination is well enough conditioned.

The effect of the orbit and clock products quality on the accuracy of the PPP provided solution is relatively easy to be checked, by comparing PPP results obtained with real-time generated products, with respect to PPP results obtained with off-line IGS-like post-processed products. One example, for the GAP1 station, located on the roof of the GMV premises at Tres Cantos, near Madrid, in Spain, is going to be shown next.

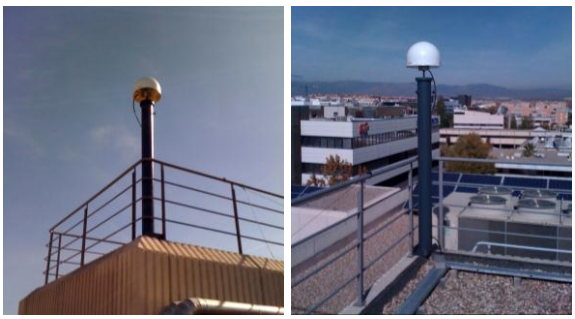

Figure 18: GAP1 Station

Figure 19: GAP1 Station Location

Figure 20 and Figure 21 below show the difference of the PPP results with respect to the pre-calibrated station coordinates, in the (North, East, Up) directions, when the PPP process is fed with real-time orbit and clock products (Figure 20), and when the PPP process is fed with off-line post processed orbit and clock products (Figure 21):

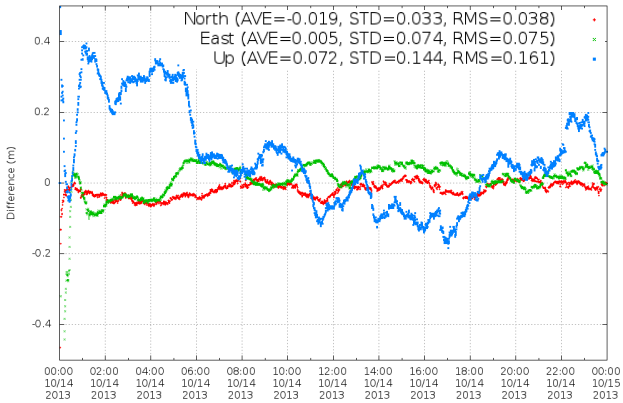

Figure 20: GAP1 station – PPP fed with real-time orbit and clock products

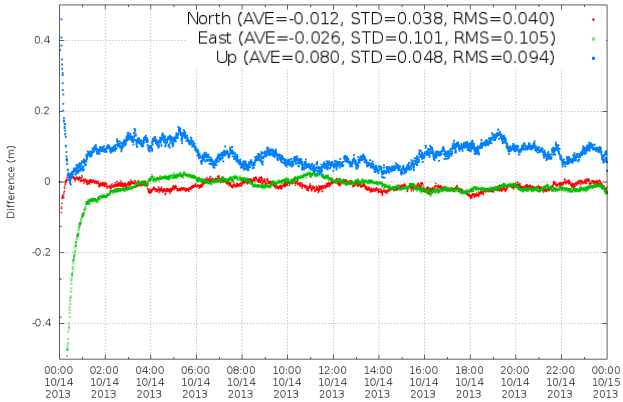

Figure 21: GAP1 station – PPP fed with off-line post-processed orbit and clock products

The RMS of the differences in the considered directions is shown in the respective plots, including the convergence period. If the convergence period is excluded, the first hour, for example, for a clearer comparison, the statistics of results of the PPP processes, in RMS, are as shown in Table 2 below:

Table 2: PPP results, difference with respect to calibrated reference position (RMS) - cm

	North	East	Horiz	Up
Real-Time	2.77	3.88	4.77	15.57
Rapid	1.55	2	2.53	8.42
Improvement	44 %	48.5 %	47 %	46 %

The table shows the differences in RMS with respect to the pre-calibrated station position, in centimetres, when real time (RT) products are used for feeding the PPP process, and when it is fed with rapid (post-processed off-line products), in each one of the north, east, horizontal (quadratic sum of the north and east components), and up directions. Performances are about a 45% better when

post-processed off-line products are used. This 45% is the theoretical maximum enhancement margin for the PPP performances, which might be reached if the real-time orbit and clock products accuracy was improved. The real improvement will obviously be smaller, even if the real-time algorithms were perfect, the products quality would still be affected by unavailability and latency problems.

It is important to be observed that the PPP estimated positions do not follow a random distribution. They are correlated to the nearby epochs, as the products errors and the geometrical conditions are. When the position error is relatively large for a certain period of time, we refer to it as an "excursion'. Excursions amplitude is usually much larger when real-time products are used for feeding the PPP processes than when they are fed with more accurate post-processed off-line products. This results in worse statistics for the real-time products fed PPP processes, when their results are compared with respect to the post-processed off-line products fed PPP processes.

We have been also trying to analyse the effect of the geometry on the PPP solutions, and we can conclude that in this case, the cause-consequence effect is not so direct.

One thing that is clear, regarding the effect of the geometry on the PPP solutions, is that the risk of inaccuracy increases as the number of satellites in view decreases. When the number of satellites in view is low, the PPP errors can grow while still keeping the PPP process residuals low. And it is only partially and indirectly through the sigma of the PPP process, that the user might be able to know that something could be threatening the PPP solution accuracy. Note that a certain advantage can be taken out of this, through the sigma of the PPP process, since it is the main contributor to one of the terms of the reliability bound computation equation, and when the geometric conditions decreases, the reliability bound increases.

Generally speaking, low visibility periods and sudden constellation configuration changes are difficult to manage by the PPP processes. Degraded geometrical conditions can result in wrong carrier phase measurement ambiguities estimation, still compatible with the rest of the PPP sequential filter parameters. This problem can only be mitigated when the number of satellites increases, making it more difficult the coexistence of compatible inaccurate parameters in the PPP process.

We have observed that the real GPS constellation, the one really affecting the *magicPPP* performances, does not provide worldwide homogeneous performances. Some figures showing the projection of the satellites at certain epoch and ground-tracks on the Earth surface, as well as the number of satellites in view and the provided PDOP (Position Dilution of Precision) values for high availability levels, in case of 0 and 1 satellite failures are presented next:

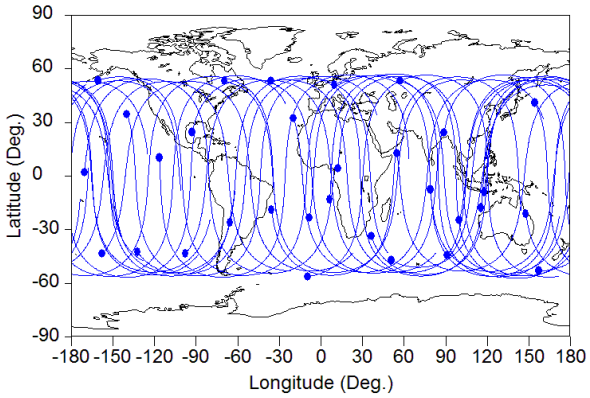

Figure 22: Real GPS Constellation SV Ground Tracks February 10th, 2014, 12:00:00 UTC + 12 hours.

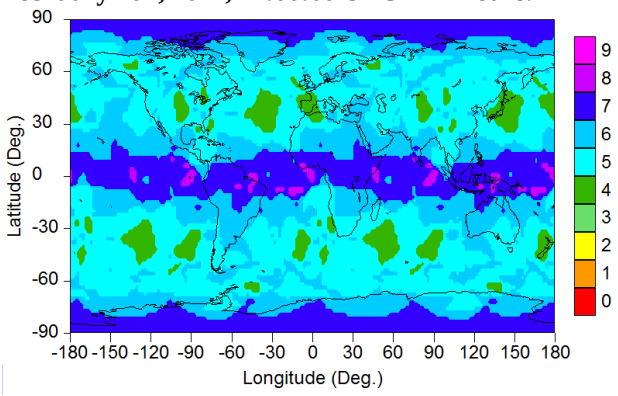

Figure 23: Real GPS Constellation – Minimum Number of Satellites in View, for 10° masking angle

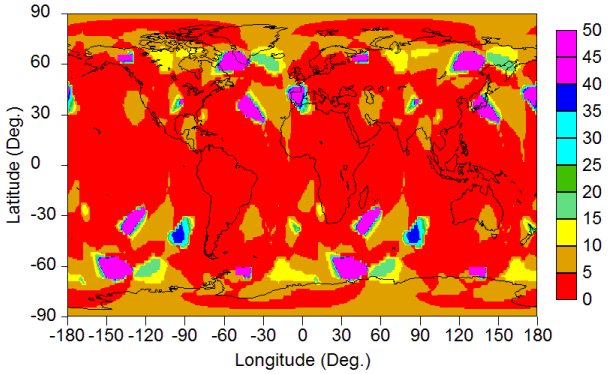

Figure 24: Real GPS Constellation – PDOP 100% availability level, 0 SV failures, 10° masking angle

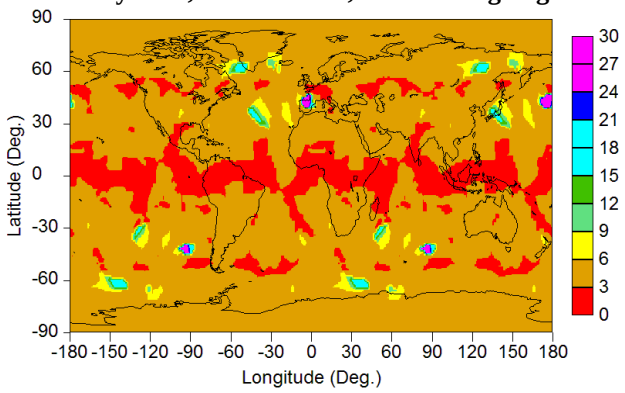

Figure 25: Real GPS Constellation – PDOP 99% availability level, 0 SV failures, 10° masking angle

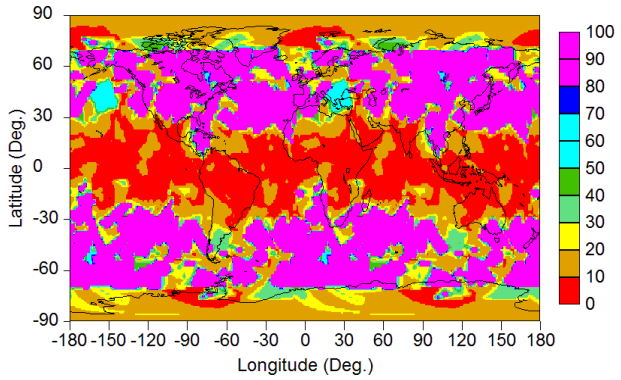

Figure 26: Real GPS Constellation – PDOP 100% availability level, 1 SV failure, 10° masking angle

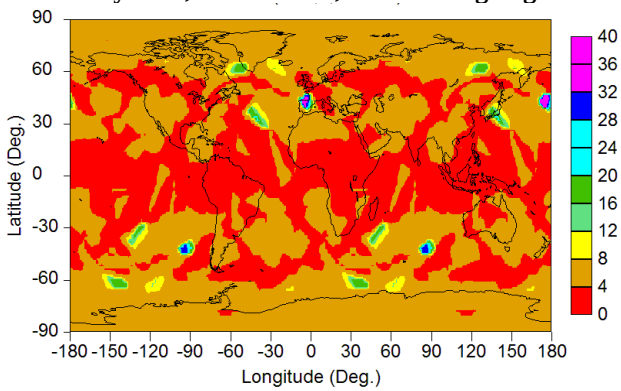

Figure 27: Real GPS Constellation – PDOP 99% availability level, 1 SV failure, 10° masking angle

The relevant aspect to be mentioned about Figure 23 above showing the minimum number of satellites in view is that in some regions in middle latitude areas, that number is as low as 4. We have already mentioned that it is risky for PPP to remain with 5 or less satellites in view. With 5 satellites in view it is really difficult to detect a faulty satellite (a satellite for which relatively inaccurate orbit and/or clock products have been computed), and with 4 it is completely impossible. Under these circumstances, any products inaccuracy is going to be directly translated into as well inaccurate PPP results. Note that the date for the analysis has not been especially chosen as a worst case. Any date between May 19th and 30th would have been worse, in terms of available satellites in view. More information about GPS satellites availability can be found in www.celestrak.com and www.navcen.uscg.gov.

The second relevant point to be observed in the figures above (Figure 24, Figure 25, Figure 26 and Figure 27) is the fact that there are 'holes' in the PDOP maps for high availability levels, i.e. there are small areas in which the PDOP values go up to extremely high values, even if those huge values are just reached for short time periods. Note that a 1% unavailability period corresponds to 14 minutes and 24 seconds, which is non negligible for a PPP process with is working 24 hours a day, providing updated positions every second. An observability problem in one of these few-minutes-long intervals can result in a discontinuity of the PPP results, which can be quickly solved or which can remain if certain not strongly constrained parameters (as it can be the case of phase ambiguities for a satellite in the initial epochs a new pass) remain coherent with a wrong position. This is the reason why relevant PDOP maps for PPP processes require 99% of 100% availability levels.

Soon the multi-constellation scene will help improving the PPP performances. Just for comparison purposes, figures analogous to Figure 23 and Figure 26 have been generated for a multi-GNSS constellation, combining the real GPS constellation with the nominal Galileo constellation (24 satellites Walker constellation, without including the 6 spare satellites, in three orbital planes, with a semi-major axis of 23,222 km, and 56º inclination, see reference [Ref. 8.]).

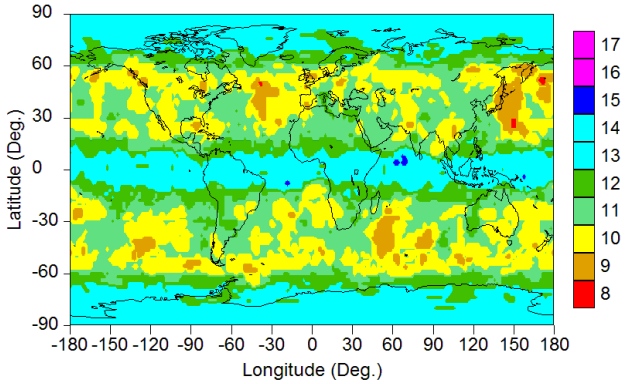

Figure 28: Real GPS + Galileo Constellation – Minimum Number of Satellites in view, 10° masking angle

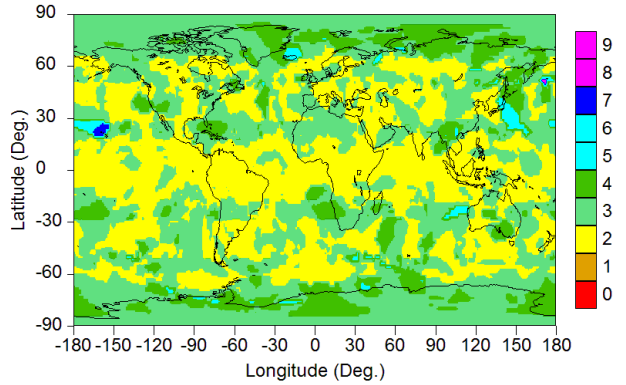

Figure 29: Real GPS + Galileo Constellation – PDOP 100% availability level, 1 SV failure, 10° masking angle

For the GPS + Galileo combined constellation, the minimum number of satellites in view is 8, and it is extremely improbable that PDOP values go beyond 5 or 6, for 100% availability level, even in the worst case of 1 satellite failure. We expect significant PPP performances improvements directly related to the imminent advent of the different multi-GNSS scenarios.

Together with this multi-constellation exercise, we have also performed another theoretical analysis, performing

an optimization of the GPS constellation. We have used *elcano*, a dedicated proprietary constellation design and optimization tool, see [Ref. 9.]. We have allowed the variation of the mean anomaly of the satellites in each one of the orbital planes, and we have obtained this way an optimized GPS constellation, able to provide enhanced geometric performances.

For illustrating the optimization, we have included Figure 30 showing the variations of the mean anomalies of the GPS satellites, together with Figure 31 Figure 32 and Figure 33, showing the optimised GPS constellation minimum number of satellites in view, and PDOP for 100% availability level, and 99% availability level, in the case of 1 satellite failure with 10° masking angle, which can be compared with Figure 23, Figure 26 and Figure 27, respectively. The comparison of the mentioned pairs of figures shows that the minimum number of satellites is never 4 in the case of the optimised constellation, and that areas in which it is 5 are relatively small, in comparison with the non-optimised case. Equivalently, the very large PDOP values obtained for large areas with the non-optimised constellation are significantly reduced after the optimization, for 100% availability level, and completely removed for 99% availability level.

It has to be remarked that this optimization is a theoretical exercise, and it is not intended to be a realistic case. However it is still interesting for illustrating the fact that the GPS constellation has some non-negligible margin for improvement in terms of geometry.

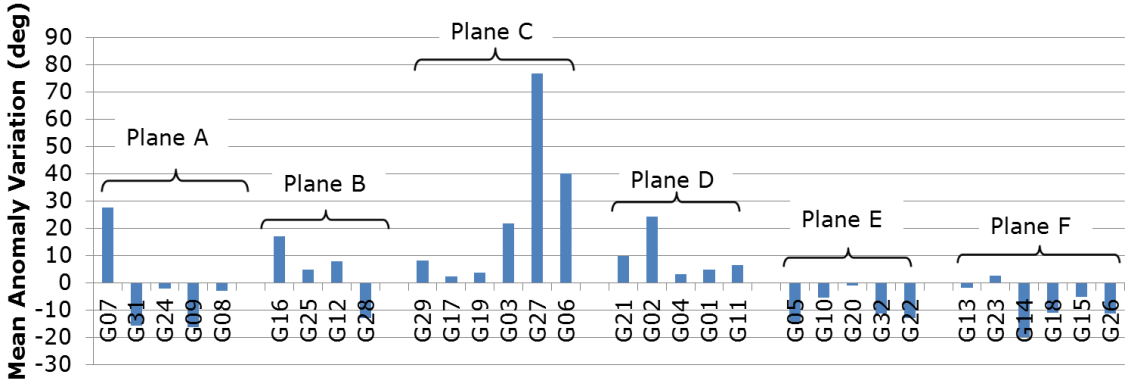

Figure 30: GPS constellation satellites mean anomaly variation

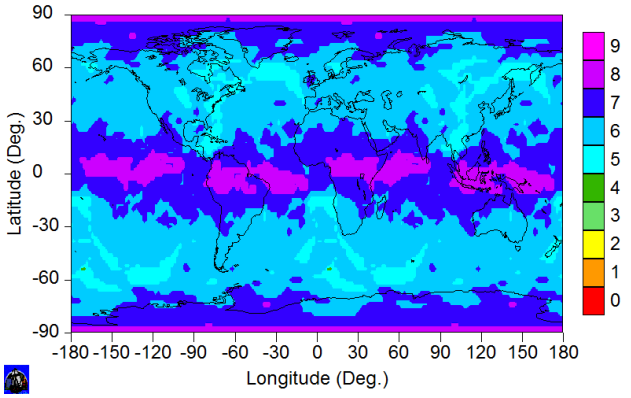

Figure 31: Optimised GPS Constellation – Minimum Number of Satellites in View, for 10° masking angle

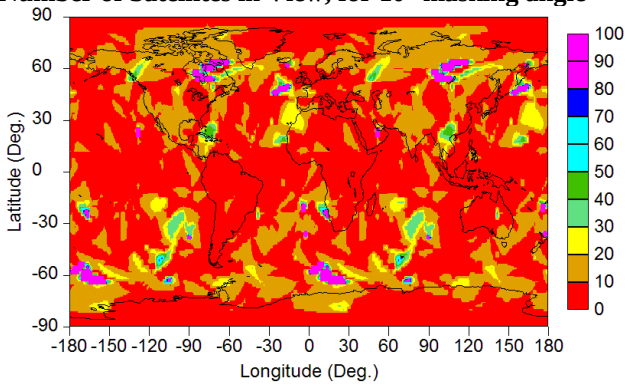

Figure 32: Optimised GPS Constellation – PDOP 100% availability level, 1 SV failure, 10° masking angle

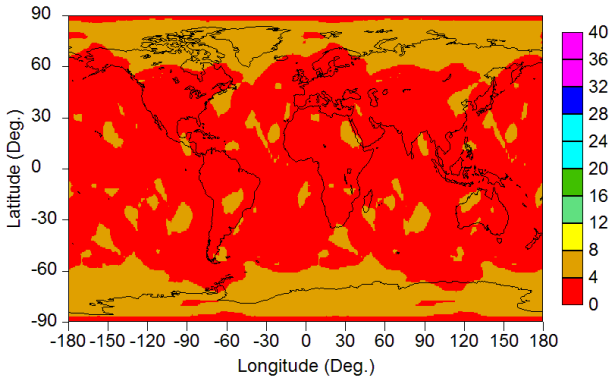

Figure 33: Optimised GPS Constellation – PDOP 99% availability level, 1 SV failure, 10° masking angle

In summary, the PPP algorithms performances for real-time open-sky scenarios are mainly limited by a combination of inaccurate orbit and/or clock products, together with 'weak' geometry conditions, whereas in partially obstructed scenarios, especially for kinematic trajectories, it is the lines of sight losses what is limiting the attainable positioning performances. Off-line processes are not affected by the limitation associated to the quality of the orbit and clock products, since the off-line generated products are usually significantly more accurate. We are going to close this section with some ideas for improvement, with the aim of overcoming the PPP processes identified limitations.

- Real time orbit and clock products generation has margin for improvement. Both orbit and clock computation processes can be optimised.
- GNSS constellation geometry will be improved in the next to come multi-constellation scenario, when Galileo and Beidou are available.
- Regional constellations, see [Ref. 7.], based on the use of IGSO (inclined geosynchronous satellite orbits) satellites for complementing the traditional MEO constellations, have the capability of providing improved geometrical conditions for the PPP processes, since IGSO satellites have the advantage of being in view for large periods of time from the target region (long IGSO passes).

In addition, there is also an additional limitation related to the fact that when all lines of sight are lost, even for a very short time period (for example when driving under a motorway bridge or passing through a tunnel), the PPP process convergence is lost, and it has to be re-started. This is especially critical in kinematic applications, when the observability conditions are more frequently and severely degraded. PPP integration with inertial sensors, and/or the implementation of a parallel mono-frequency PPP process can help overcoming this continuity problem in severe or moderate obstructed scenarios, respectively.

Regarding the PPP process convergence period, several approaches are being investigated by different PPP expert teams. One alternative for the convergence period reduction is the implementation of an integer ambiguity fixing approach, which requires the calibration of certain biases for which a denser tracking network is needed, as well as additional bandwidth. This is an intermediate strategy between standard PPP without integer ambiguity fixing and RTK. Convergence time can be reduced, but it is not instantaneous, and yet it adds an extra dependency on auxiliary infrastructure. Another alternative that can be investigated for reducing the convergence time is the implementation of a mono-frequency PPP process, fed with parameters from an atmospheric model, for the initialization of the standard PPP process. By now, what we have already incorporated in *magicPPP*, is a 'quick-start' initialization mode, which can be directly applicable in many applications. This mode consists of feeding the PPP with a pre-calibrated position (provided by static PPP or saved from a previous work session), which allows the PPP process to start from a converged point. Further information about this 'quick-start' feature can be found in [Ref. 5.].

Finally, for the enhancement of reliability bound computation, we can suggest the inclusion of the not yet considered term related to the indirect geometry and products quality motorization through the observation of the PPP solution at a pre-calibrated position. In case of relatively large discrepancies, the reliability level can be increased accordingly, for adding robustness to the process. Note that, unlike for RTK, there is no rigid requirement about the relative distance between the pre-calibrated station and the PPP user. There might be a slight reduction of the advantage with respect to RTK associated to the additional dependency on certain infrastructure elements, but almost negligible, since baselines of hundreds of kilometres would still be acceptable. This improvement has been implemented and tested. The obtained results are reported subsequently, in section 'Improved *magicPPP* reliability bound'.

RELATIVE PPP AND CLARIFICATIONS FOR PPP/RTK COMPARISON

RTK (Real Time Kinematic) is a differential positioning method, developed in the early 1990's, based on the use of dual-frequency carrier phase measurements of the GNSS signals where a base station receiver at a well-known, calibrated location transmits signal corrections in real time to one or several rover receivers. RTK is a technique employed in applications where precision is mandatory; it is not only used as a precision positioning tool, but also in automatic machine guidance activities such as precision farming. RTK corrections compensate atmospheric delay, orbital and clock errors, etc., increasing relative positioning accuracy up to the centimeter level. However the absolute position is accurate only to the level of the computed or known position of the base station. The positioning determination process begins with a preliminary ambiguity resolution, which allows almost instantaneous convergences. In practice, convergence is not always quick and perfect. As the distance with respect to the base increases, or in relatively unstable atmospheric conditions, the accuracy of the ambiguity fixing process degrades. Under these circumstances, ambiguities are sometimes inaccurately fixed. The computed values might be showing a stable behavior, and so the positioning solution, when suddenly a discontinuity takes place, when new ambiguity fixes are found. It can sometimes take a few minutes to get the right values. RTK processes usually have a quality indicator, which can be used for knowing whether the provided solution can be considered to be converged. RTK correction data is typically sent via UHF or spread spectrum radios that are built specifically for wireless data transfer. The corrections from the base station receiver can be sent to an unlimited number of rovers.

One of the main limiting factors of RTK is the maximum distance, in terms of acceptable performances, between the base station and the rover, so it implies having a rather large density of base stations to ensure a proper coverage in large areas. The variability of both the troposphere and the ionosphere introduces systematic errors which limit this maximum allowable distance for obtaining precise positioning to 10 or 20 km. In order to tackle this distance problem, the concept of Virtual Reference Station (VRS) was introduced in the year 2000 [Ref. 1.], and the Wide Area RTK (WARTK) concept was introduced in the late 1990s [Ref. 2.]. VRS allows performing RTK positioning in reference station networks with distances of up to 40 km. The idea is to generate Virtual Reference Stations

which simulate a local base station close to the user receiver. Thus, the errors cancel out better than by using a more distant base station. However, even 40 km distance between base stations may still imply a rather large station density for big areas. WARTK allows the extension of local services based on the real-time carrier phase ambiguity resolution to wide-area scale (i.e. baselines between the rover and reference stations greater than 100 km), for both dual-frequency (only GPS) and 3-frequency systems (also with Galileo and modernized GPS). The Wide-Area Real-Time Kinematics (WARTK) technique for 2 and 3-frequency systems are based on an optimal combination of accurate ionospheric and geodetic models in a permanent reference stations network. The main techniques supporting WARTK are related to an accurate real-time computation of ionospheric corrections, combined with an optimal processing of GNSS observables (carrier phases in particular) in both 2 and 3-frequency systems. The method increases the RTK/NRTK service area, with permanent stations separated by up to 500–900 kilometers. Although its feasibility has been demonstrated with real data, no WARTK operational system has been deployed so far.

It is important to be remarked that PPP provides absolute positioning, whereas RTK provides relative positioning. As stated before, with RTK, the provided absolute position is accurate only to the level of the computed or known position of the base station.

PPP is not a differential technique, but still it could be interesting to make some quick analyses in order to get some information about whether it would have sense to think of a relative PPP process, and what its performances would be. The test was carried out using data for May 5th, 2014. The PPP solution for GAP1 station showed a relatively large 'excursion' that date, on the vertical component, between 14:00 and 18:00 hours, and we were interested in getting to know if simultaneous PPP processes for other stations in the surrounding of the considered GAP1 station would show a similar behaviour.

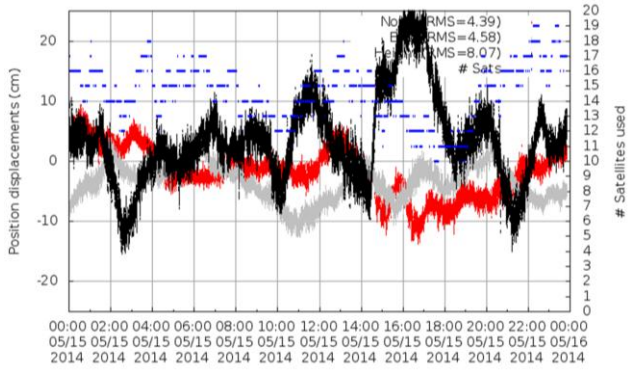

Figure 34: PPP solution for GAP1 – May 5th 2014.

Five additional stations have been included in the analysis: MAD2, VILL, YEBE, EBRE and MEDI. Approximate coordinates and location for the considered stations are provided in Table 3 and Figure 35 below:

Table 3: Considered stations coordinates

Station	Latitude (N) – deg	Longitude (E) - deg
EBRE	40.82	0.49
GAP1	40.59	356.29
MAD2	40.43	355.75
MEDI	44.48	11.63
VILL	40.44	356.05
YEBE	40.52	356.91

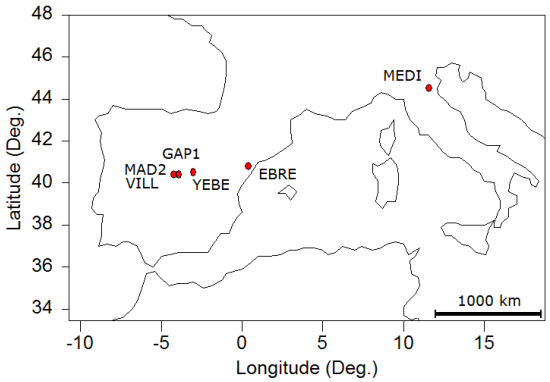

Figure 35: Considered stations location

Analogous PPP processes have been carried out for the six considered stations. Four of them are relatively near to GAP1, whereas EBRE is about 800 km away, and MEDI is about 2800 km away. Note that the considered stations are equipped with different receiver and antenna types, for excluding potential receiver processing correlations. The vertical component has been compared among the different processes, and the results for the PPP absolute positioning process are presented in Figure 36 below. The difference between with the obtained PPP positions and the calibrated reference positions for each one of the considered stations is shown for the vertical component:

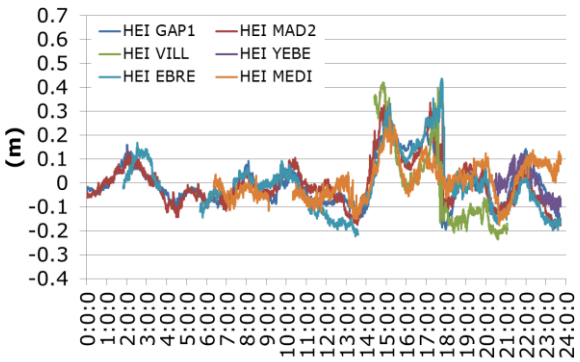

Figure 36: Absolute PPP solutions – May 5th 2014 – vertical component.

The coherency of the obtained results shows that some relative PPP technique could make sense to be used with the aim of trying to compensate for the geometry/products quality combination errors. The performed analysis is very limited, for the short considered time period, and reduced number of stations, but still seems promising. Just for adding some context information, we include the following information: the minimum number of satellites in view from the GAP1 station was 4, at about 19:40,

whereas the minimum number of satellites in view from the MEDI station was 6 all through the considered day.

In view of the obtained results, it can be concluded that a PPP based relative technique would work, and would provide reasonable results, even in no so short baselines. Providing corrections for a few hundreds of kilometres baselines would still be feasible. However we are not going to apply the obtained results for trying to improve the accuracy of the PPP processes. We intend to use it for improving the PPP reliability bound computation instead. Our objective is to enhance the reliability computation algorithm by building a dedicated term, generated at server level, able to indirectly measure the quality of the orbit and clock products provided to the PPP process and the constellation geometry.

IMPROVED *magicPP*P RELIABILITY BOUND

The initial approach to the reliability bound computation was defined based on the following assumptions:

- It is necessary to account for the fact that PPP techniques are providing **absolute positioning** and not relative positioning. This implies that some errors may be coming from the lack of definition of the terrestrial reference frame.
- The **covariance** indicators coming out from the PPP estimation filter implemented at user level must be taken into account. It should be noted that those indicators are based on some hypothesis that may not be always confirmed, and consequently some margins may be added to provide a reliable protection level.
- The **residuals** coming out from the position estimation process, mainly those provided for the phase measurements, are providing very valuable information. This is particularly relevant in urban areas or areas affected by poor visibility conditions. It should be noted that the phase residuals are typically below 1.5 cm and the fact that they are be very sensitive to any positioning error.
- The **quality of the PPP products**, orbits and clocks, must be considered. The PPP service provider must consequently transmit a parameter indicating the quality of the products to be generated.
- During the **convergence** period, some additional margins should be added to be able to compensate for the strong initial correlations between the different parameters.

All the mentioned factors were considered in the initial algorithm, see [Ref. 6.], except for the one related to the quality of the PPP products. In a first approach, we thought we could monitor the quality of the orbit and clock products, at server level, individually, for each one of the GNSS satellites. Our intention was to detect "faulty" satellites, which might degrade the PPP performances, In order to exclude them for the PPP process. But then we realised that it was not possible to identify particular "faulty" satellites. Satellites with significant problems are rejected in the OD&TS process, and are obviously not used in the PPP processes, but in other cases, small inaccuracies are spread all through the OD&TS process. We think that these small inaccuracies, which cannot be traced to individual satellites, are what cause the previously mentioned "excursions" in the PPP solutions. So the initial reliability algorithm has been enhanced taking into account additional information from the server, which can monitor the difference between a calibrated position and the PPP provided solution, and use it as an indirect indicator of the quality of the orbit and clock products. Note that we are no providing any reliability bound value for epoch at which the number of satellites in view is 5 or lower.

Next, some examples are going to be shown, illustrating the improvement of the PPP reliability bounds when using the enhanced reliability computation algorithm.

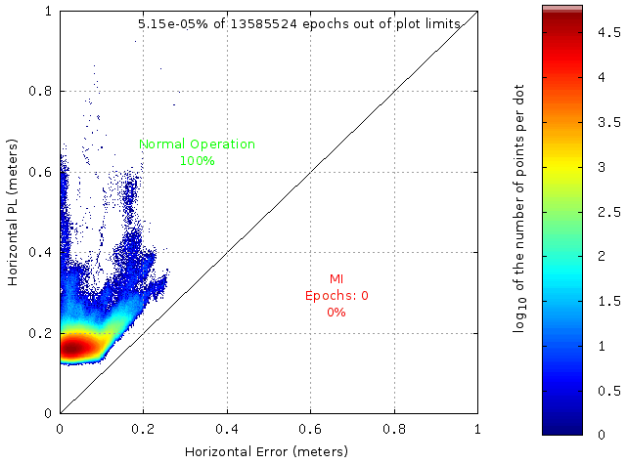

Figure 37: Improved PPP reliability algorithm, horizontal component - Stanford diagram

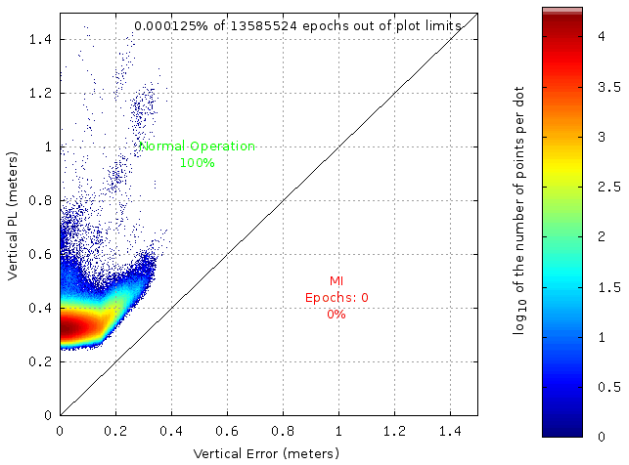

Figure 38: Improved PPP reliability algorithm, vertical component - Stanford diagram

Figure 37 and Figure 38 show that the improved reliability algorithm is able to cope with all the integrity failures which were not able to be correctly managed by the previous algorithm.

Further improvements are foreseen, especially for more challenging partially obstructed scenarios, in which the main limitation is not related to the products quality but to the line of sight loss. Complementary adapted RAIM (Receiver Autonomous Integrity Monitoring) techniques could be of great help in these environments.

CONCLUSIONS

- PPP is consolidating as an alternative/complementary to RTK high positioning technique.
- PPP is able to work in static and kinematic scenarios, both in real-time and in post-processing modes, for many different highly demanding applications.
- PPP positioning performances are better than 10 cm (horizontal) and better than 15 cm (vertical), 95%, after 20 minutes convergence period.
- The high accuracy of the PPP solutions and the robustness for the PPP processes have allowed the definition of a promising improved reliability bound computation algorithm.
- The provided reliability bounds are in the range of a few decimeters, without providing integrity failures in the analysed scenarios.
- There is still margin for improvement (geometry, orbit and clock products quality, convergence, robustness in partially obstructed scenarios, etc.).

REFERENCES

[Ref. 1.] Vollath, U., Deking, A., Landau, H., *Long-Range RTK Positioning Using Virtual Reference Stations*, ION GNSS 2000.

[Ref. 2.] Hernández-Pajares Manuel, et al, *Application of ionospheric tomography to real-time GPS carrier-phase ambiguities resolution, at scales of 400-1000 km and with high geomagnetic activity*, Geophysical Research Letters Vol. 27(13), pp. 2009-2012, 2000.

[Ref. 3.] Píriz, R., Mozo, A., Navarro, P., Rodríguez, D., "magicGNSS: Precise GNSS Products Out of the Box," *Proceedings of the 21st International Technical Meeting of the Satellite Division of The Institute of Navigation (ION GNSS 2008)*, Savannah, GA, September 2008, pp. 1242-1251.

[Ref. 4.] Píriz, R., Calle, D., Mozo, A., Navarro, P., Rodríguez, D., Tobías, G., "Orbits and Clocks for GLONASS Precise-Point-Positioning," *Proceedings of the 22nd International Technical Meeting of The Satellite Division of the Institute of Navigation (ION GNSS 2009)*, Savannah, GA, September 2009, pp. 2415-2424.

[Ref. 5.] Mozo, Álvaro, Calle, J. David, Navarro, Pedro, Píriz, Ricardo, Rodríguez, Daniel, Tobías, Guillermo, "Demonstrating In-The-Field Real-Time Precise Positioning," *Proceedings of the 25th International Technical Meeting of The Satellite Division of the Institute of Navigation (ION GNSS 2012)*, Nashville, TN, September 2012, pp. 3066-3076.

[Ref. 6.] Samper, M. D. Laínez, Merino, M. M. Romay, "In-The-Field Trials for Real-Time Precise Positioning and Integrity in Advanced Applications, *"Proceedings of the ION 2013 Pacific PNT Meeting"*, Honolulu, Hawaii, April 2013, pp. 146-167.

[Ref. 7.] Laínez, M.D., Romay, M.M., "OD&TS Process Evolution Based on Interoperability Between Different Navigation Satellite Systems, *"Proceedings of the 22nd International Technical Meeting of The Satellite Division of the Institute of Navigation (ION GNSS 2009)*, Savannah, GA, September 2009, pp. 1504-1518.

[Ref. 8.] ESA Navipedia, European Space Agency. navipedia.net

[Ref. 9.] http://www.gmv.com/en/space/Satellite_navigation_systems/GNSS_tools_development.html

[Ref. 10.] RTKLIB by Tomoji Takasu (*gpspp.sakura.ne.jp/rtklib/rtklib.htm).*